Pergamon

Int. J. Solids Structures Vol. 35, Nos 31–32, pp. 4147–4166, 1998

0020–7683/98 $19.00 + .00

PII: S0020–9683(97)00307–7

STRAIN LOCALIZATION—SHORT TO LONG CORRELATION LENGTH TRANSITION

DUSAN KRAJCINOVIC
Mechanical and Aerospace Engineering, Arizona State University, Tempe AZ, U.S.A.

and

MILENA VUJOSEVIC*
Technology and Product Development, Sensor Product Division, Motorola, Phoenix AZ, U.S.A.

(*Received* 27 *November* 1996; *in revised form* 15 *May* 1997)

Abstract—The current study considers the problem of the strain localization as being a dynamic transition in the range of the correlation length. Using the particle dynamic method within the framework of statistical physics the proposed model re-examines the assumptions and simplifications of the traditional, quasi-static, continuum localization theories. Special attention is focused on the softening regime, "mystery" of the vanishing fault width and the reasons for this "pathological" result. The proposed model suggests an objective and physically acceptable measure of the fault "width". © 1998 Elsevier Science Ltd. All rights reserved.

1. BACKGROUND

Analytical modeling of the seemingly instantaneous qualitative changes in the deformation field of solids, subjected to the displacement controlled conditions, developed in the last two decades into a fascinating field of the applied mechanics research. In a seminal study of the localization of plastic deformation Rice (1976) identified the loss of homogeneity as a common thread relating the formation of Luders bands in metals, "cross slip" in crystals, coalescence of cavities or voids into bands (void sheets), shear bands in clay shale and faulting in rocks. Rice (1976) also demonstrated that the transition (bifurcation) from a state of a homogeneous strain field to a state of non-homogeneous strain field (characterized by the very large strains localized within a very small fraction of the specimen volume) belongs to the class of Hadamard's instabilities of the material constitutive description. The sage advises that the continuum estimates of the conditions leading to the localization "depend critically on subtle features of these (constitutive) descriptions" and that "the role of deformation field non-uniformities or imperfections ... seem often to be of great importance" (Rice, 1976) did not have a perceptible restraining effect on the subsequent analytical and computational studies of localization. Furthermore, the thought that the arguments related to the vanishing width of the shear band (fault) or to the pinpointing of the onset of localization may be the consequence of the inherent limitations of the static, deterministic, local continuum models was seldom seriously entertained.

The scarcity of the non-deterministic models of the localization in mechanical systems (with the exceptions of Lockner and Madden 1991; Delaplace *et al.*, 1996) is even more surprising in view of the existence of the condensed matter physics models that deal with a class of conceptually similar phenomena. In particular, Anderson (1958) demonstrated that the localization of electron waves within a small part of the specimen in an essential manner depends on the phenomenon kinetics and microstructural disorder. The objective of the present study is to reconsider the strain localization phenomenon from a statistical viewpoint and the particle dynamics model. The narrow goal of this study is to replicate in a

* Author to whom correspondence should be addressed.

qualitative sense the salient aspects of the localization phenomenon, softening response and explore the non-deterministic role of the microstructural disorder.

2. PHENOMENOLOGY OF FAULTING IN ROCKS

Owing to the large features of its microstructural texture the tests on rock specimens are very useful in the study of the localization statistics. With some insignificant alterations cylindrical rock specimen is initially subjected to a hydrostatic pressure which is kept fixed for the test duration. Subsequently, the specimen is monotonically and quasi-statically contracted (in a displacement controlled condition) along its axis. It is interesting to mention that the first studies of the considered phenomena, disguised as the brittle to "ductile" transition, can be traced to von Karman (1911) in order to explain the stress–strain curves for Carrara marble specimens. These early phenomenological studies suggested that the specimen response is "ductile" if it can "sustain permanent deformation without loosing its ability to resist loads" (Jaeger and Cook, 1979). In contrast, the response is brittle (specimen "softens") if the deformation can increase at decreasing stresses. If the stress–strain curves are plotted in the $\sigma_{ax}-\sigma_{lat}$ vs ε_{ax} space (where indices "ax" and "lat" refer to axial and lateral components of two tensors) the brittle–ductile transition is defined as the smallest shear at which the curve exhibit the tendency to soften (Patterson, 1978, etc.). The proposed criteria turned out to be reasonably correct even though the arguments were based on the ductility which is seldom found in rocks.

The first well documented test of the micromechanical type, conducted by Hallbauer *et al.* (1976) on quartzite specimens, provides the photographs of the specimen cross sections and careful estimates of the crack density at ten different states along the specimen stress–strain curve. More recently, Lockner, *et al.* (1991) and Lockner and Byerlee (1992) conducted a similar series of tests on several different rocks. These results were discussed and compared to the existing micromechanical models by Reches and Lockner (1994). A record of the acoustic emission (AE) data for several segments of the deformation process is from the viewpoint of this study the principal advantage of this series of tests.

Each AE signal is related to a transient elastic wave generated by a rapid conversion of the cohesive (surface) energy into a kinetic energy of atoms related to the separation of two adjacent sheets of atoms (formation of an internal surface or crack that supports the discontinuity in the displacements) within the specimen. A crack propagates if the consecutive AE are bunched closely together near its front (tip). In contrast, the damage evolution is controlled by the crack nucleation if the AE locations are randomly distributed over the specimen volume. The ability to distinguish between these two principal modes of damage evolution; namely, the nucleation and propagation of cracks, is critical for the study of localization.

The Reches and Lockner (1994) discussion of the AE data can be summarized as follows: (a) microcrack induced damage remains diffuse until the peak stress, (b) prior to the fault nucleation the AE activity is slow and uniformly distributed throughout the specimen, (c) location of the fault nucleus cannot be detected from the precursor AEs, (d) the most intense AE activity is recorded at the front of the propagating fault and (e) the pattern of the fault propagation (from it nucleus) and the existing damage incurred prior to the fault nucleation are not correlated (refuting the assumption that the fault grows as a result of its coalescence with the preexisting cracks in its path).

3. MICROMECHANICS OF FAULTING

The AE test supported synopsis of the mechanics of faulting, inferred from the Reches and Lockner (1994) discussion of the test data recorded in the course of a comprehensive experimental program, can be interpreted micromechanically as follows:

(i) During the initial phase of deformation the damage evolution is controlled by the microcrack nucleation attributed to the short range tensile stresses (such as Hertzian stresses at the contact of two grains in limestone) at many randomly located sites [see (a) above].

In the absence of long range tensile stresses and substantial shear stresses the propagation of already nucleated cracks is prevented by the negative stress intensity factors (SIF).

(ii) As the process of nucleation continues the crack density increases and the distance separating the adjacent cracks decreases. Near the peak of the specimen stress–strain curve [see (a) above] the interaction of few closely spaced cracks may render their SIFs positive. The crack propagation commences when the interaction amplified SIF of a small ensemble of closely spaced cracks (fault nucleus) becomes large enough to satisfy the Griffith's condition. The biasing effect of the interactions maintains a statistical preference for angles of 65–60° between the normal to the crack bedding plane and the specimen axis. The site at which the fault is nucleated is obviously random [see (c) above] since the precise location of the first stress amplifying interaction between two neighboring cracks during a random nucleation process is a variate.

(iii) The propagation of the fault is dominated by the cooperative effect, i.e. the interaction induced crack growth [see (d) above]. The rate of the fault growth is typically rapid since the disordering effect of the crack growth increases at the expense of the ordering (mean field) effect of the crack nucleation. In other words, once the statistical homogeneity is lost on a small scale the attendant stress concentrations tend to promote the loss of the homogeneity on a larger scale. The rate of this "avalanche" effect, manifested on the specimen scale as the slope of the softening segment of the force-contraction curve depends on whether the material is damage sensitive (micro-homogeneous) or damage tolerant (micro-heterogeneous) (Krajcinovic, 1996), lateral confinement, details of the experimental set-up, kinetics of the imparted energy, etc.

According to the available evidence the exact location and time of the fault nucleation cannot be pinpointed neither in tests nor by analyses. The exact point at which the loss of homogeneity occurs depends on the selected criteria and is, therefore, a matter of speculation. Softening phase is not limited to the strain localization. In damage tolerant materials, subjected to tensile tractions, localization may occur well before one of the defect clusters transects the specimen (Hansen *et al.*, 1989; Krajcinovic and Basista, 1991). In this case (typical for composite materials) the loss of the specimen homogeneity near the peak of the stress–strain curve is attributed to the stress concentrations in the neighborhood of several large crack clusters (nether one of which spans the specimen). The dominant role of the extreme statistical moments of the stress distribution renders the data computed from the mean field based analytical models unreliable.

4. THERMODYNAMIC STATE AND ITS CHANGE

A volume of a material with a heterogeneous microstructure is referred to as being statistically homogeneous (Kreher and Pompe, 1989; Krajcinovic, 1996; i.p.) if the statistical properties of all relevant random fields are independent of the local fluctuations locations (translational invariance). The smallest volume within which the material and specimen response are statistically homogeneous is referred to as the representative volume element (RVE). In the process of the homogenization the effective properties of the RVE are assigned to the corresponding material point of the continuum. A volume of a material with a heterogeneous micro-structure is referred as being statistically self similar (Krajcinovic, 1997) if it is scale invariant. Finally, a material is on the observed scale non-local if the strain in a material point depends not only on the stress in the same point but also on the stresses within an arbitrary non-zero domain of influence.

For the purpose of stress analysis a body is often partitioned into sub-volumes (such as the finite elements). The discretization is mesh-independent (objective) only if the response and material of each sub-volume is statistically homogeneous (i.e. at least as large as the corresponding RVE). The thermodynamic state of a sub-volume changes both quantitatively and qualitatively during a deformation process characterized by the evolution of damage (see the above discussion of tests by Lockner *et al.*, 1991). As long as the crack concentration remains dilute and the damage evolution controlled by crack nucleation an initially homogeneous rock specimen remains homogeneous. Occasional interaction between two isolated microcracks has a negligible effect on the sub-volume homogeneity

and macro-response. The AE signals recorded in a test during which the homogeneity is preserved are randomly distributed over the entire specimen.

As the density of the nucleated cracks increases they randomly form many small clusters. An ensemble of the closely spaced (correlated) cracks will be defined as being a cluster if its growth is initiated and sustained by the direct interaction of constituent cracks. A cluster can also be formed by intersecting or concatenated cracks. As soon as the first cluster is formed the relative contribution of the crack growth to the damage evolution increases at the expense of the crack nucleation. Eventually one of the clusters (referred as being a fault) becomes dominant. The strain localized in the fault is much larger than the strain in the rest of the specimen which relaxes elastically. Further deformation is attributed to the declining fault shear stiffness caused by the rupture and rotations of relatively slim (and poorly constrained) fault bridging segments. The AE activity is very intensive at the fault perimeter since the elastic energy is concentrated near the tips of the growing cracks belonging to the fault. The material within the fault is, therefore, neither statistically homogeneous nor self similar. The relaxed material in the exterior of the fault remains statistically homogeneous (Finno *et al.*, 1996) and its response linearly elastic.

The question whether the material on the specimen scale is statistically homogeneous depends on the fault size. An appropriate measure of the cluster (fault) "size" is, in the analogy to the percolation theory, the correlation length. Without getting too subtle about the details the correlation length ξ can be defined as being proportional to the fault length (measured in the direction of its propagation), i.e. the size of the region of topologically different material. Rigorously, the clusters longer than ξ are exponentially rare (Isichenko, 1992). The effective properties and constitutive descriptions of the materials in the exterior and the interior of the fault cannot be identical. The question how large the parameter ξ must be before the structure and response of the entire specimen becomes inhomogeneous can be answered only indirectly by stating that a statistically homogeneous specimen cannot soften. The negative ratio of the rates of volume averaged axial stresses and strains $(d\sigma/d\varepsilon) < 0$ renders the velocity of the stress waves propagation imaginary. Since the stress waves do propagate through the specimen it follows that the specimen cannot be statistically homogeneous within the softening regime. Hence, the loss of homogeneity or localization can occur either within the hardening regime or at the peak of the force-elongation curve.

The upper bound on the onset of the localization can be defined quantitatively as $\xi \to L^-$, where L is the linear size of the specimen. The specimen is statistically homogeneous when the condition $\xi \ll L^-$ is satisfied. Correspondingly, the condition $\xi \approx L^-$ must be satisfied within the softening regime. The correlation length ξ can be, at a given state, determined experimentally by plotting the distribution of distances $L_{i,i+1}$ separating pairs of consecutively AEs (Lockner and Byerlee, 1992; Delaplace *et al.*, 1996). Defects are not correlated if any distance $L_{i,i+1}$ is equally possible since the nucleation controlled damage evolution is characterized by a random distribution of the distances between the pairs of consecutive AEs; namely, $p(L_{i,i+1}) = \text{const}$. The frequency of small distances $L_{i,i+1} \approx L_0$ (of the order of the resolution length L_0) increases if the damage evolution is controlled by the growth of cracks forming the fault. The correlation length can be estimated from the crossover between the random distributions $p(L_{i,i+1}) = \text{const}$. and $p(L_{i,i+1}) \neq \text{const}$. that characterizes larger frequency of small distances between consecutive AEs (Delaplace *et al.* 1996).

The distance $L^{\min}_{i,i+1}$ between the new AE and the closest already recorded AE can also be used to distinguish different modes of damage evolution during different phases of the deformation process. In general, the frequency of clusters is always inversely proportional to the cluster sizes. However, the exact form of the proportionally rule depends on the damage density and evolution mode and microstructure (thermodynamic state) of the material.

5. DETERMINISTIC MODELS OF LOCALIZATION

From the phenomenological and deterministic viewpoints of the traditional continuum mechanics the onset of localization in a specimen, subjected to a uniform, quasi-static stress

field, is defined as a bifurcation from a state of a homogeneous strain field to a state of a strongly localized strain field. A majority of the available continuum models are based on the hypothesis that the localization may be viewed as an instability of the macroscopic constitutive description of the inelastic deformation of the material (Rudnicki and Rice, 1975; Rice, 1976). The onset of the localization can be within this scheme determined from the constitutive description of the material at the state of incipient bifurcation. As a result, localization is an intrinsic (material) failure mode since its threshold is defined by an intensive parameter which depends on the volume averaged fields that characterize the material macroscopic response and is independent of the specimen mass (size).

The traditional continuum model, based on Hadamard's stability theory (Hill, 1963), defines the conditions at which the strain rates become discontinuous along the interfaces of a thin band (fault) that instantaneously bisects the specimen subjected to the uniform, quasi-statically and monotinically increasing displacement. Following Ottosen and Runesson (1991), Bigoni and Hueckel (1991) and Neilsen and Schreyer (1993) the Maxwell's compatibility conditions require that the strain rate in the exterior (superscript "o") and interior (superscript "i") of the localized band are related as

$$\dot{\varepsilon}^{\mathrm{i}} = \dot{\varepsilon}^{0} + \dot{\varepsilon}^{\mathrm{d}} \tag{1}$$

where

$$\dot{\varepsilon}^{\mathrm{d}} = \tfrac{1}{2}(\dot{\mathbf{m}} \otimes \mathbf{n} + \mathbf{n} \otimes \dot{\mathbf{m}}) \tag{2}$$

is a kinematically admissible discontinuity in the strain rate across the band perimeter, $\dot{\mathbf{m}}$ a vector co-directional with the relative velocities on the two sides of the interface separating the localized band from the rest of the specimen and $\mathbf{n}$ the unit vector normal to the band. Symbol $\otimes$ stands for the dyadic (outer) product of two vectors.

The constitutive relation between the rates of macro stresses and macro strains is

$$\dot{\sigma}^{\mathrm{i}} = \mathbf{D}^{\mathrm{i}} : \dot{\varepsilon}^{\mathrm{i}} \quad \text{and} \quad \dot{\sigma}^{0} = \mathbf{D}^{0} : \dot{\varepsilon}^{0} \tag{3}$$

where $\mathbf{D}$ are the effective tangential stiffness (elasticity) tensors for the interior and exterior of the band. The dots (colon) in (3) define the scalar (inner) tensor product.

The continuity of tractions normal to the band boundaries requires that

$$\mathbf{n} \cdot (\dot{\sigma}^{\mathrm{i}} - \dot{\sigma}^{0}) = 0 \tag{4}$$

Combining eqns (1)–(4) and assuming that the two tangential stiffness tensors $\mathbf{D}^{\mathrm{i}} \equiv \mathbf{D}^{0}$ are equal at the incipient bifurcation, it follows that

$$\mathbf{Q} \cdot \dot{\mathbf{m}} = 0 \tag{5}$$

where

$$\mathbf{Q} = \mathbf{n} \cdot \mathbf{D}^{\mathrm{i}} \cdot \mathbf{n} = \mathbf{n} \cdot \mathbf{D}^{0} \cdot \mathbf{n} \tag{6}$$

is the second order acoustic tensor.

The expression (5) is satisfied if and only if the acoustic tensor has at least one zero eigenvalue, i.e. if

$$\det \|\mathbf{Q}\| = 0 \tag{7}$$

Mathematically, the condition (7) is interpreted as the loss of ellipticity associated with the zero eigenvalue of the tangential stiffness tensor $\mathbf{D}$. The normal $\mathbf{n}$, that corresponds to the zero eigenvalue, defines the band slope, i.e. the angle subtended by the contraction axis

and the fault perimeter. As a consequence of (7) the elastic shear waves are trapped at the fault perimeter since their speed $c_t = \sqrt{G_t/\rho}$ vanishes (Wu and Freund, 1984). The symbol G_t represents the effective shear modulus and ρ the mass density.

Despite their utility and mathematical elegance the traditional, local plasticity models lead to a non-physical behavior which was summarized by Simo (1989) who stated that "strain localizes to a set of measure zero ... (and) ... the classical local dissipation becomes meaningless since no dissipation can take place in a localized set of zero Borel measure ... (such that) numerical simulation of softening exhibits a totally spurious mesh dependency".

Further development of the continuum models are due to Needleman (1988, 1989) who considered the rate dependent constitutive description of the material. To resolve the problem of mesh-dependence and vanishing thickness of the fault Bazant and Pijaudier-Cabot (1988) formulated a non-local hardening model, Aifantis (1984), Triantafyllidis and Aifantis (1986). Muhlhaus and Aifantis (1991), de Borst and Muhlhaus (1992) and Vardoulakis and Aifantis (1994) a gradient-dependent continuum, Muhlhaus and Vardoulakis (1987), Sulem and Vardoulakis (1990) and de Borst (1991) a micro-polar continuum. Billardon and Doghri (1989) and Rizzi (1995) considered the degradation of stiffness due to the accumulating damage, introduced graded materials while Peric *et al.* (1993) considered cohesionless geomaterials. DiLellion and Olmstead (1997) determined the evolution of the shear band width using the boundary layer theory (needed to provide a characteristic length) in conjunction with the continuum model. Finno *et al.* (1996) studied the response within the band in sands. Frantziskonis and Loret (1995) considered the application of wavelet analysis to localization. Numerical remedies associated with mesh dependence and zero thickness of the localized band were suggested by Needleman (1989), and Belytschko and Lasri (1989) and others. Finer points of the model related to the boundary conditions were discussed by Benallal *et al.* (1990). As predicted by Rice (1976) embellishments of the constitutive law were more than sufficient to fit any test result. Moreover, as suggested by Simo (1989) all those "seemingly different approaches ... (are) ... different manifestations of the same basic notion" and are based on "a non-local regularization of the dissipation function of the continuum model".

A comprehensive review of the localization literature is well beyond the scope of this paper. A vast majority of continuum models provide valuable insights into various aspects of the localization phenomena. According to local, deterministic, phenomenological and continuum theories localization takes place in a zero volume. Hence, the question whether the material within the band is homogeneous or not is not an issue. Existing non-local models assume that a single length suffices for the description of the interaction between closely spaced cracks. However, a complete statistical description of the interaction of two crack-like defects involves distributions of distances between two isolated points, an isolated point and a point on the periphery of a crack, and two points on the peripheries of two adjacent cracks. The corresponding n-point correlation functions are discussed and defined in Torquato (1991) and probability functionals in Kreher and Pompe (1989). Construction of these functions is an arduous task that requires time and effort.

Two-dimensional micromechanical models of the formation of the shear (crack) band were formulated on the basis of the linear elastic fracture mechanics and mean field theory by Horii and Nemat-Nasser (1986), Isida and Nemat-Nasser (1987), Sammis and Ashby (1986), Fleck (1991) and others. In all of these cases the actual stochastic geometry is approximated by a homogeneous solid weakened by a periodic arrangement of slits of equal size and shape centered along a straight line at an angle to the compression axis. In a succinct review of the first three papers Wong (1990) concluded that the proposed models simultaneously exaggerate the effect of interaction and overestimate the stabilizing effect of the lateral confinement. Furthermore, a self-similar evolution of damage (that preserves the periodicity of the defect arrangement needed for the application of the cell model) provides an upper bound on the energy needed for failure (Bazant and Cedolin, 1991; Krajcinovic, 1996). It is notable that these micromechanical models assume that an array of slits that spans the specimen already exists in the specimen and that the fault propagates in the direction of its width. This assumption is contradicted by the AE tests and conclusions in Reches and Lockner (1994). Fine tuning of deterministic models is a perilous task in

view of the sensitivity of the localization onset on the details of the constitutive description. The particle dynamics simulations, that emphasize the statistical aspect of the phenomenon, show that a simple model may, indeed, suffice to replicate the general trends observed in tests. Two types of models are complementary since the simulation results can be used to formulate the constitutive laws of analytical models.

6. DISCRETE MODEL

A lattice formed by a homogeneous ensemble of interacting discrete masses lumped in nodes is a realistic and physically correct model of a solid only on the atomic scale. However, in many cases these lattices provide a qualitatively accurate picture of damage evolution in solids with a disordered microstructure on a much coarser scale. For example, the intergranular cracking of a two-dimensional ceramic "specimen" subjected to the tensile tractions can be modeled by a triangular lattice (Delaunay lattice) which is dual to the Voronoi tessellation of grain boundaries (Fig. 1). Each link of the lattice corresponds to the grain boundary that is perpendicular to it. The stiffness and strengths of links can be derived from the elastic parameters of the ceramic. Denoting by f_i and f_{ci} the force in the link and the link rupture strength, the link "i" ruptures when the criterion

$$f_i = f_{ci} \tag{8}$$

is satisfied.

The quenched disorder (related to the different grain sizes and the presence of interfacial residual stresses or phases of different tensile strength) is introduced by selecting appropriate distributions of link lengths and strengths (Krajcinovic, 1996). The simulations are rather simple and consist of the repetition of the sequence to two steps: determination of forces in the links of the lattice and the removal of the link for which the condition (8) is satisfied. Damage in the form of links removed from the Delaunay lattice corresponds to the debonded grain facets in the Voronoi tessellation (Fig. 1). In the case when the lattice is subjected to the tensile tractions the links that carry largest loads are dual to the grain boundaries that are sub-normal to the maximum tensile stresses. The corresponding damage pattern (cracked grain boundaries) fits the data observed in tests. This is not true when a lattice is subjected to the compressive nodal forces. The remedies suggested by Schlangen and van Mier (1992), Tzschichholz *et al.* (1994), Jirasek and Bazant (1995) for frozen (static) lattices are not entirely satisfactory (Krajcinovic, 1996).

The damage evolution in a specimen subjected to compressive tractions can be simulated efficiently and correctly replacing the "frozen" lattices by the particle dynamics model (based on the molecular dynamics formalism, see, for example, Allen and Tildesley, 1994). The two-dimensional specimen made of a generic brittle material is in this study approximated by a topologically perfect triangular lattice in which all masses, except of those at

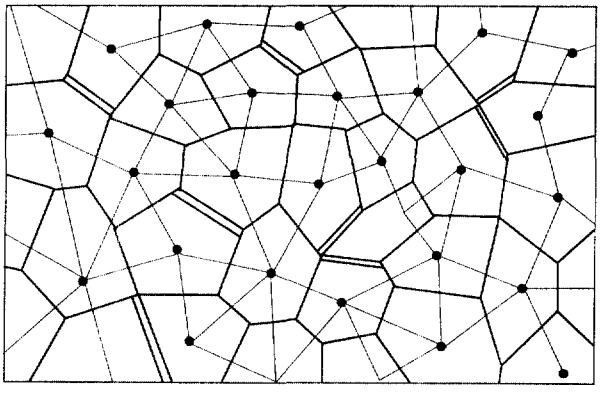

Fig. 1. Voronoi tessellation and the Delaunay lattice.

the external surfaces, are linked to six of their nearest neighbors. The geometrical disorder of the lattice is simulated by selecting the normal probability distribution of links lengths within the band $(0.1L_0,\ 1.9L_0)$. Link stiffnesses are assumed to be equal while the link tensile strengths are uniformly distributed within the band $(0, f_{ci}^{\max})$. The overall lattice shape was selected to fit the 2.5 width to length aspect ratio of the specimens tested by Lockner *et al.* (1992). The mass of the specimen is lumped into 3535 particles, located in lattice nodes, arranged into 101 rows of 35 particle each.

In analogy to Lockner *et al.* (1992) tests the lattice is initially subjected to the biaxial compression which is kept fixed for the test duration. Subsequently, the lattice is monitonically and quasi-statically contracted in the axial direction (under deformation controlled conditions). After each quasi-static increment of the externally applied contraction the system is allowed to relax into a state characterized by an arbitrarily chosen but infinitesimally small level of kinetic energy. The simulations were carried out through the hardening and softening regime and were interrupted well into the post-softening regime.

7. RESULTS OF NUMERICAL SIMULATIONS

The macroscopic and microscopic features of the deformation obtained by particle dynamics simulations are strikingly similar to the corresponding features observed in tests by Hallbauer *et al.* (1976) and Lockner *et al.* (1992). The macroscopic curve relating the axial force F and the specimen axial contraction u, obtained in simulations, is plotted in Fig. 2c. For convenience the force F is divided by the lattice width B while the contraction is divided by the lattice length L. Six characteristics states, marked by t_i $(i = 0, 5)$, are located within the hardening, softening and post-softening regimes. The deformed specimen and the distribution of ruptured links at state t_5 are shown in Fig 2a and b.

The principal objective of the particle dynamics simulations is to examine the statistics of the damage evolution, range within which the specimen is statistically homogeneous, range within which the local continuum models are valid and geometry and kinematics of the fault. Comparisons with the tests are of a qualitative nature since the lattice is, in contrast to the test specimen, two-dimensional and since its parameters were not determined from the macroscopic parameters of the rock specimens used in the referenced tests.

The evolution of the damage is depicted in the top row of Fig. 3. The dots in each of the six blocks define the links ruptured within the range $t_i - t_{i+1}$. The total damage can be determined superimposing all six blocks to compare the simulations of this study with acoustic emission tests from Lockner *et al.* (1992) (shown in y–z and y–x planes in the two bottom rows of Fig. 3). The patterns and kinematics of the damage evolution observed in localization tests and simulations exhibit identical trends (except in the part of the volume adjacent to the interface with the load transfer device in tests). The damage evolution along the hardening segment of the force-concentration curve is distributed homogeneously over the entire specimen. The localization of the damage (AE signals) into the fault takes place somewhere along the softening regime (between states t_3, t_4).

The angle of the fault can be estimated from the distances of pair events within the regime in which the fault growth is most pronounced (between states t_3 and t_4 in Fig. 2). These averages, measured in the x and y directions and non-dimensionalized by dividing them by the average link length, were $\langle \lambda_{i,i+1}^{x} \rangle = \langle L_{i,i+1}^{x}/L_0 \rangle \approx 9.35$ and $\langle \lambda_{i,i+1}^{y} \rangle \approx 13.88$, respectively. Hence, the averaged angle β subtended by the contraction axis y and the fault perimeter is

$$\beta \cong \arctan \frac{\langle \lambda_{i,i+1}^{x} \rangle}{\langle \lambda_{i,i+1}^{y} \rangle} = 34^{\circ} \tag{9}$$

Further insight into the localization is provided by the plots of the strain distribution shown in Fig. 4. The strain within the hardening (state t_1) is obviously homogeneous. Small local fluctuations are randomly dispersed over the entire surface of the lattice. Several bands, bedded in planes at approximately $\pm 30^{\circ}$ from the contraction axis, are evident at

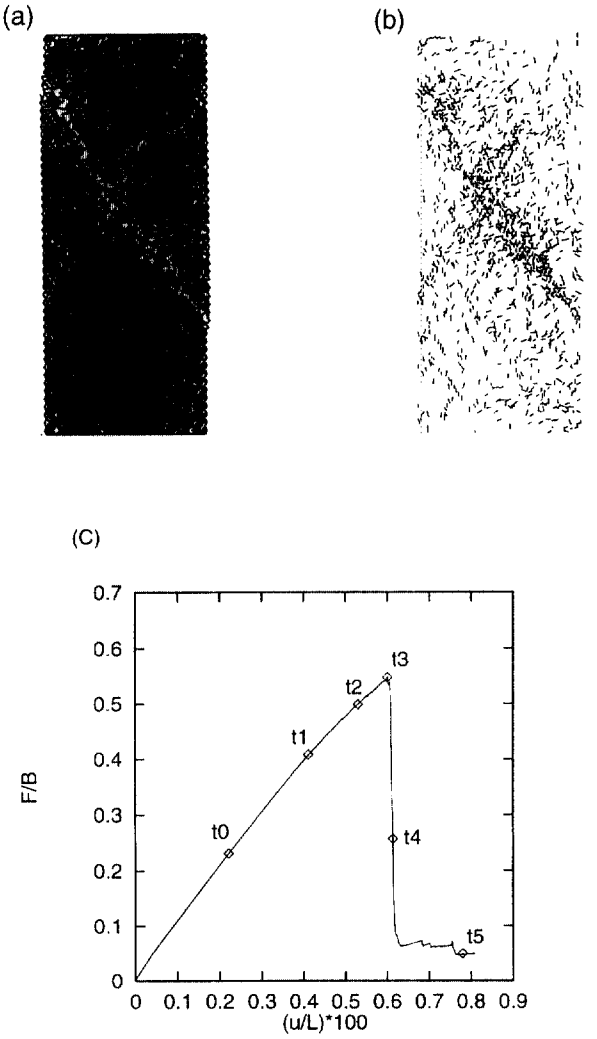

Fig. 2. (a) Deformed specimen configuration (state t_5). (b) Crack distribution in state t_5. (c) Axial force vs. displacement curve.

the peak of the force-contraction curve (state t_3). None of these bands is long enough to violate the homogeneity conditions $\xi < L$ (Krajcinovic, 1997) on the specimen scale. However, the distribution of link forces is multifractal (Hansen *et al.* 1989; Krajcinovic, 1996) and the macro-response is influenced if not entirely dominated by the set of these clusters. The response on the specimen scale cannot remain homogeneous along the softening (state t_4) and post-softening (state t_5) regimes. The deformation is in these two states dominated by a single fault. In keeping with the conclusions in Reches and Lockner (1994) the exact band which will develop into the fault cannot be singled out on the basis of the morphology of the precursor states including the one at the top of the force-contraction curve.

The damage evolution mode can be inferred from the distribution $p(\lambda_{i,i+1})$ of distances $\lambda_{i,i+1}$ between the locations of two consecutively ruptured links (i.e. AE signals). When the distances between pairs of consecutive AE signals are randomly distributed, i.e. when $p(\lambda_{i,i+1}) = \text{const.}$, the specimen remains homogeneous (Lockner and Byerlee, 1992; Delaplace *et al.*, 1996). The defects are not correlated and the damage evolution is dominated by the crack nucleation. The histogram of minimal distances $\lambda_{ij}^{\min}$ between a new AE signal and the already recorded signals provides a measure of the width of largest cluster.

The histograms of lengths $\lambda_{i,i+1}$ and $\lambda_{ij}^{\min}$ are plotted in Fig. 5 for the four states marked on the force-specimen contraction curve in Fig. 2. To interpret these histograms it should

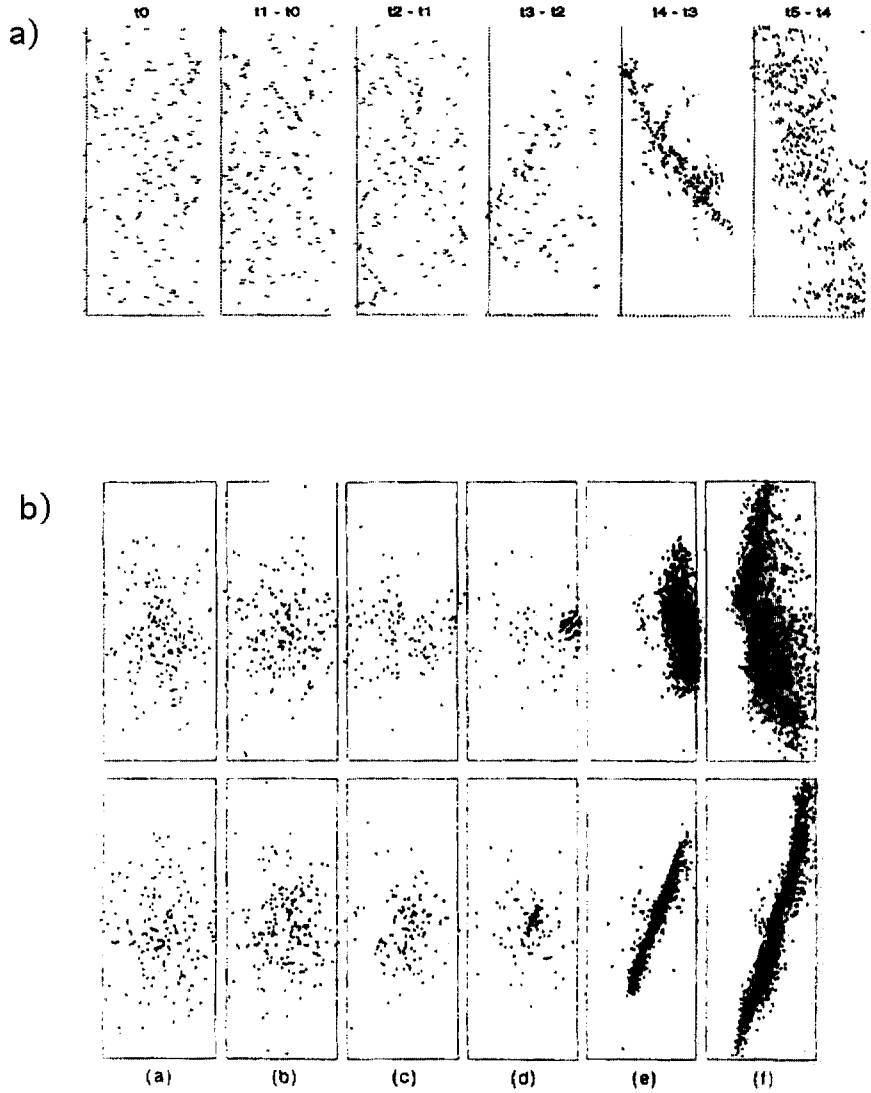

Fig. 3. Spatial distribution of defects at different deformation stages according to the simulations (top row) and experiments (Lockner and Byerlee, 1991).

be kept in mind that the bin's width is 0.5. The minimum normalized distances between the centers of two diagonals and between a diagonal and a horizontal link joined at a node are 0.5 and 1.0 between two horizontal links. The histogram that shows the frequency of distances $\lambda_{i,i+1}$ (Fig. 5a) indicates that the state t_0 is homogeneous and that the response is dominated by the crack nucleation (weak links). The preponderance of small distances $\lambda_{i,i+1}$ increases as the specimen contracts reflecting the gradual shift to the crack propagation mode and the increasing effect of the crack interaction on the damage evolution (cooperative effect). The histogram on Fig. 5b demonstrates that the total number of small distances between two ruptured links (AE signals) grows at the expense of large distances as the significance of crack propagation (ruptures due to the stress concentrations—hot spots) on the damage evolution increases at the expense of the defect nucleation (ruptures of weak links). Depending on the selected criterion the fault "width" can be from the Fig. 5b estimated to be anywhere from 2.5 to $4L_0$. Since the localization is not an instantaneous transition neither tests nor simulations data provide an exact state at which the bifurcation from the statistically homogeneous to a statistically inhomogeneous state takes place.

Continuum models of the strain localization are based on the assumption that the onset of the localization can be determined from the condition (7), i.e. from the effective

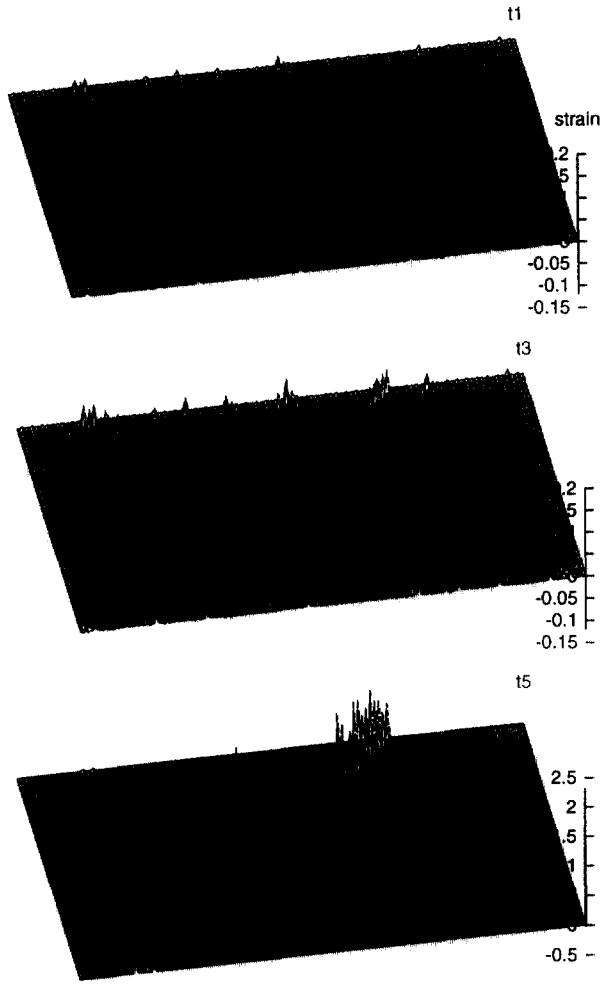

Fig. 4. Strain distribution in states t_1, t_3 and t_5.

parameters of the statistically homogeneous material. The acoustic tensor can be determined from (6) for any statistical homogeneous state for which the components of the effective tangential stiffness are known. For a given state of damage the tangential lattice stiffness was determined from $C'_{ijmn} = \mathrm{d}\sigma_{ij}\,\mathrm{d}\varepsilon_{mn}^{-1}$ by imparting a strain $\mathrm{d}\varepsilon_{mn}$ (to the already faulted lattice) and determine the corresponding stress increments $\mathrm{d}\sigma_{ij}$ (while all other components of the strain tensor are equal to zero). The determinant of the acoustic tensor (normalized by division with the link stiffness k) was computed for all orientations in ten different states (Fig. 6) and plotted in Fig. 7. Figures 2 and 6 represent two physical realizations of the same statistics.

In the initial state (slightly damaged by the presence of the zero strength links) the minimum of the acoustic tensor determinant occurs along the shear planes $\beta = \pi/4$ as expected for an isotropic, homogeneous, elastic continuum subjected to biaxial compression. As the damage grows the angle at which the $\det\|\mathbf{Q}\|$ is at minimum swings towards the contraction axis. At the peak of the force-concentration curve the angle β subtended by the contraction axis and the $\det\|\mathbf{Q}\|$ is minimum in a plane subtending the angle of 34° with the contraction axis (Fig. 8). As a result of disorder the acoustic tensor never vanishes as suggested by continuum prediction (7). However, the angle at which the acoustic tensor for a given state is minimum ($\beta \approx 34°$) is in excellent agreement with the continuum prediction and the values obtained from the consideration of the correlation length (9). A line of this slope is superimposed on the defects accumulated during the entire hardening regime in Fig. 8 to underline this agreement.

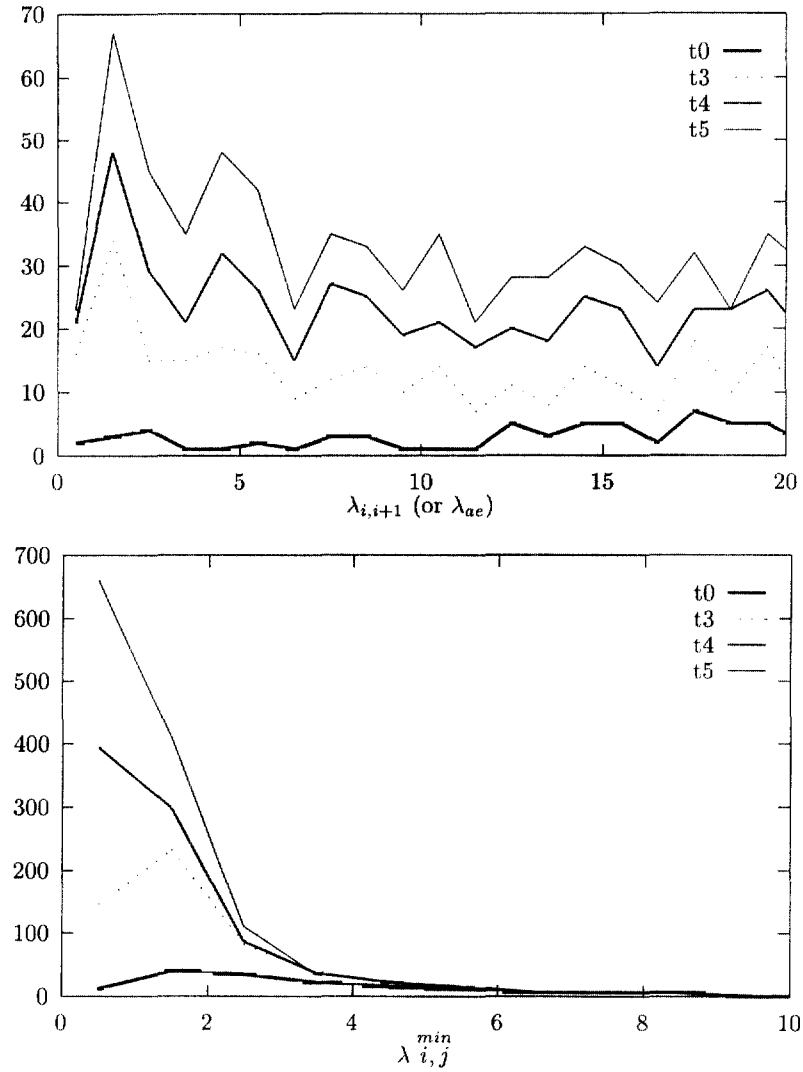

Fig. 5. (a) Histogram of distances separating pairs of successively broken bonds. (b) Histogram of distances separating a newly nucleated defect from the closest existing defect.

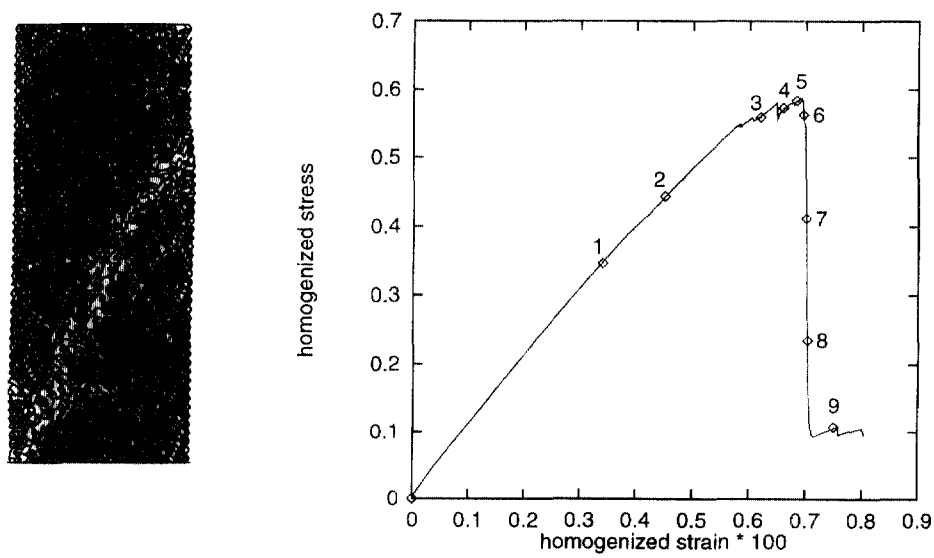

Fig. 6. Specimen configuration at the state 7 and the corresponding force-specimen contraction curve.

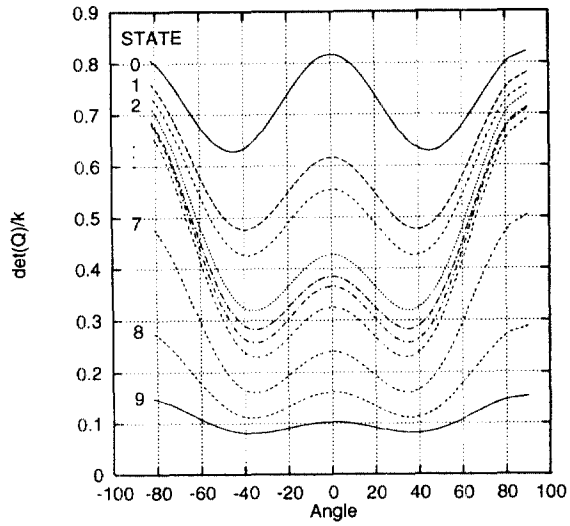

Fig. 7. The determinant of the acoustic tensor plotted against the angle measured from the specimen axis. The determinant is evaluated for states 0 to 9 shown in Fig. 6.

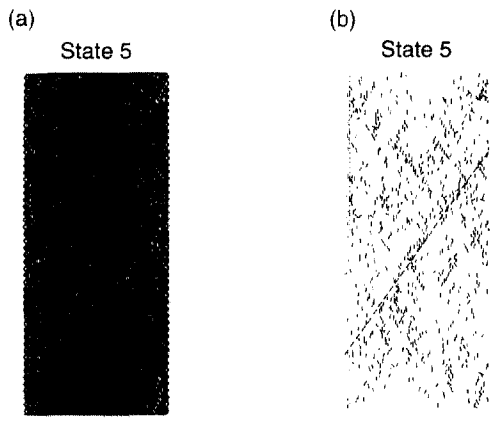

Fig. 8. (a) Specimen configuration at the peak of the force-contraction curve (state 5). (b) Defects configuration in state 5.

In the softening and post-softening regimes the angle at which the $\det\|\mathbf{Q}\|$ is minimized starts swinging back towards $\beta = \pi/4$. This pathological behavior of the acoustic tensor, that reflects the loss of the accuracy of deterministic and local continuum models, are directly related to the fact that the faulted specimen is not statistically homogeneous.

The rate at which the non-dimensionalized minimum value of the acoustic determinant $\kappa(Q) = \min\|Q\|/\min\|Q_0\|$ declines with respect to the axial strain is shown in Fig. 9a. The plots of axial, lateral and shear components of the effective stiffness tensor vs the axial contraction are plotted in Fig. 9b. In both cases the stress–strain curve is added by a dotted line for the orientation. It is important to note that the volume averaged components of the effective tensor start misbehaving in the softening regime, i.e. in the aftermath of the peak of the stress–strain curve. Therefore, the volume averaged components of the stress and strain tensors cease to be a realistic measure of corresponding fields.

The geometry (size) of a fault is important in earthquake, mining, petroleum, civil and geomechanical engineering. For a variety of reasons the analytical and computational determination of the fault width proved to be a very elusive goal. A thought that the fault width is a material parameter has been supported by many authors. Roscoe (1970) claimed that the fault width is a material parameter which can be defined "as a small multiple of the mean grain size". Bazant and Cedolin (1991) concluded that the width ranges from 2–

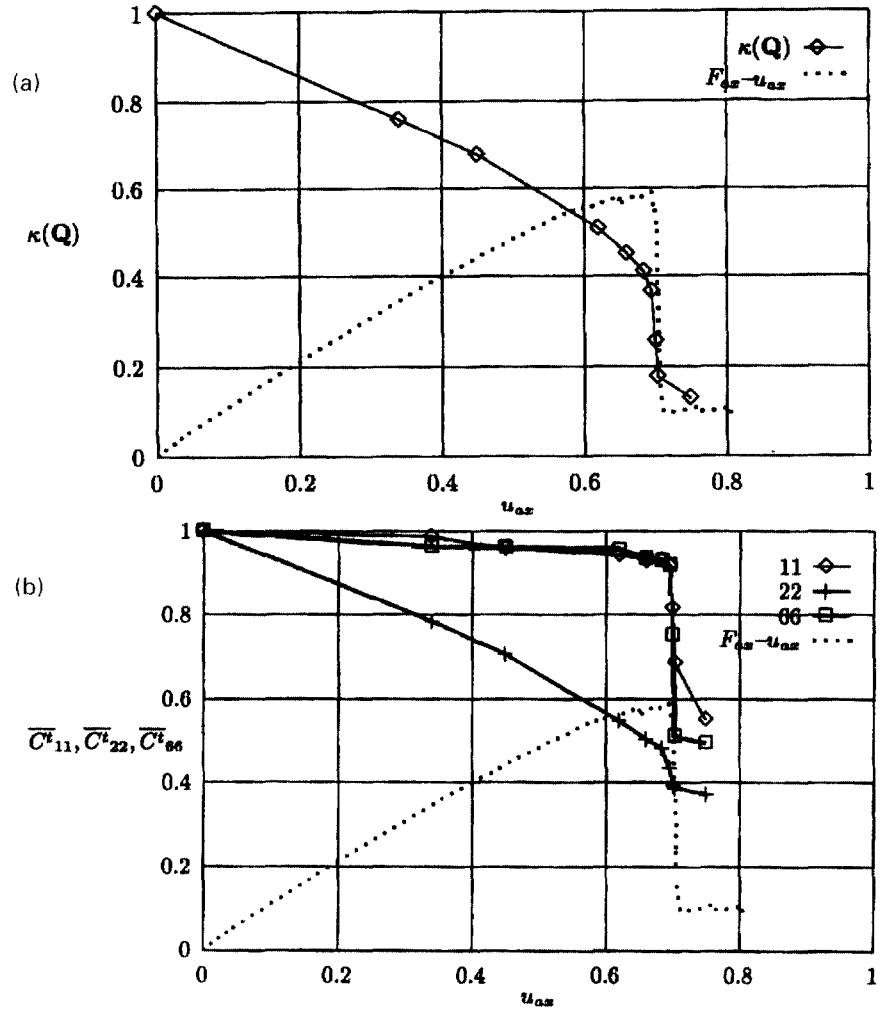

Fig. 9. (a) The normalized minimal values of the acoustic tensor determinant $\kappa = \min[\|Q_{ik}\|]$ plotted vs. the axial displacement for ten states in Fig. 6. (b) Diagonal components of the effective tangential stiffness tensor plotted vs. axial displacement.

8 times maximum aggregates size $d_{\max}$ with an "overall optimum" of $3d_{\max}$. In rocks the fault width, according to the same source, was found to be $5d_{\max}$. Vardoulakis and Graf (1985) and Vardoulakis *et al.* (1985) estimated the fault width to be 16 times the mean grain size d_{mean} for medium grained sands. Larger multiple of d_{mean} for the fault width in sands (in comparison to concrete and rocks) is related to the smaller shear strength (cohesion) of sand and was, in fact, reproduced analytically (using a Cosserat model) by Muhlhaus and Vardoulakis (1987). The dependence of the fault width on the microstructural texture (grain or imperfection) length was also advocated by Loret and Prevost (1990) in localization in elastic–(visco)–plastic solids, Belytschko *et al.* (1991) and Frantziskonis and Loret (1995) in visco-plastic solids. One of the problems with this measure of the band width is that the texture "length" is almost always a distribution of lengths that can never be described by a single parameter.

The truth is, nevertheless, even more complex. As the experiments (Hallbauer *et al.* 1976; Lockner *et al.* 1991, etc.) and present simulations indicate the faults in rock specimens with a disordered microstructure are of irregular shapes. In all cases the "interface" separating the interior of the fault from the exterior is blurred. The perceived fault width is biased by the adopted criterion and dependent on the resolution length of the eye, measuring device or model. It seems that the geometry of the shear band cannot be uniquely determined since the individual cracks forming the fault do not touch or intersect.

In summary, the geometry of the interface separating the interior of the fault from its exterior depends on the adopted criterion, characteristic lengths and damage tolerance (band-width of the distribution of microstructural energy barriers, Krajcinovic, 1996) of the material. The influence of the strain rate, temperature (Vujosevic and Krajcinovic, 1997) and specimen geometry (van Mier, 1984) on the band geometry should not be dismissed either.

The basic premise of the argument developed in this study is that the problem of fault geometry in general, and its width in particular, cannot be settled by a tape measure alone. The degree to which two cracks interact depends not only on the geometry (distance and orientation) but also on the damage affected local stress fields. Hence, a purely geometrical observation provides but a partial description of the fault size. Finally, a geometrical measure of the fault width changes along its length and varies from one physical realization of some statistics to the other.

To be useful a fault "width" must be identifiable, measurable and universal. The universality of the "measure" is manifested by the robustness of the measure, i.e. its independence of the details of microstructure that cannot be replicated in tests and simulations. Instead of measuring the geometry which is almost always hidden within the specimen it seems more productive and reasonable to determine the fault "width" by measuring its effect on the effective transport properties of the specimen.

Since there is no assurance that the material within the fault is either statistically homogeneous or statistically self-similar many analytical and computation models of the traditional mechanics are not useful in estimating the "true" geometry of the fault. However, the experimental determination and analytical estimates of the specimen (extensive) properties (such as the effective diffusivity or stiffness) are relatively simple tasks. Moreover, there is always a fair chance that a universal scaling law for the fault width may exist despite the obvious disorder and the fact that the details of the fault geometry change from one physical realizations of same statistics to the other.

Since the process of localization is stochastic, universal measures of the deformation are important for the interpretation of the test data. For example, the propagation range of an elastic p-wave initiated in a point of a homogeneous (or weakly disordered) solid is asymptotically proportional to the time (Sahimi, 1994). Elastic waves propagate in homogeneous solids to very large distances in the absence of scattering. The propagation of elastic waves through a strongly disordered solid is quite a bit different. For example, it was found that the electron waves may be either localized over an atomic-scale region or extended over large macroscopic-scale (Anderson, 1958). It is important to note: (a) that the localization is impossible in the absence of disorder and (b) that the localization range depends on the frequency and energy of electron waves.

The diffusion on and vibration of randomly diluted (disordered) lattice in the asymptotic neighborhood of the percolation threshold are reviewed in Stauffer and Aharoni (1992) and Sahimi (1994). The relation between the two phenomena (Sahimi, 1994) leads to a very elegant procedure for the determination of universal parameters of the system at the imminent localization. However, the analytical forms of these scaling laws were derived for the case when the percolation cluster (formed by defect nucleation) has a well defined mass and when the microstructure within the cluster is self-similar (scale invariant) as the result of the random dilution (crack nucleation). In the considered case of localization the fault grows through crack interaction and does not have a well defined mass. The material in the fault "interior" is neither statistically homogeneous nor self-similar (since the distribution of the damage, driven by the interaction induced growth of cracks, is not random) rendering the derivations in Sahimi (1994) inapplicable.

In the absence of a reliable analytical method the effective parameters of the damage non-local materials must be determined by numerical simulations. Consider first the propagation of elastic p-waves through a specimen spanned by a fault (shown in Fig. 2). The wave propagation velocity of the material decreases as the damage accumulates. A p-wave imparted to the top of the faulted specimen will, therefore, need more time to arrive to the bottom than the identical wave imparted to the top of the pristine specimen. The time lag is proportional to the fault "width" and the proportionality constant is related to the decrease of the axial stiffness of the heavily damaged material within the fault.

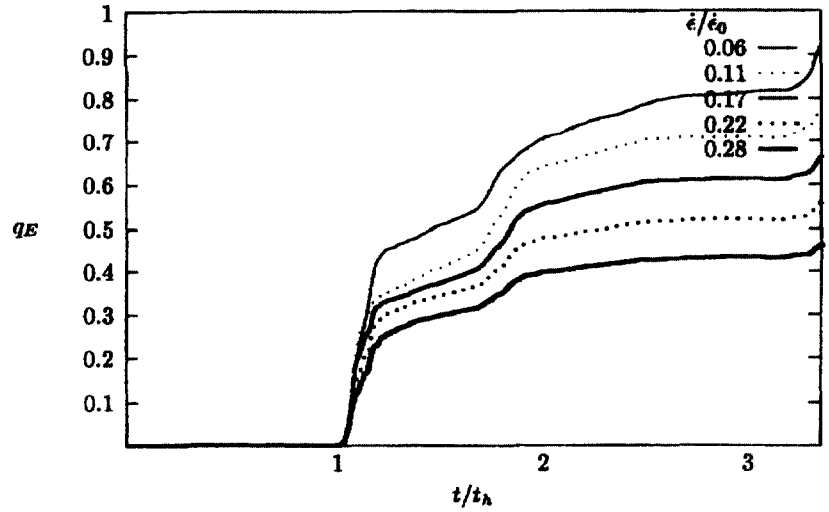

Fig. 10. Fraction of the externally imparted elastic strain energy that arrives to the bottom of the pristine specimen plotted vs. time for six strain rates.

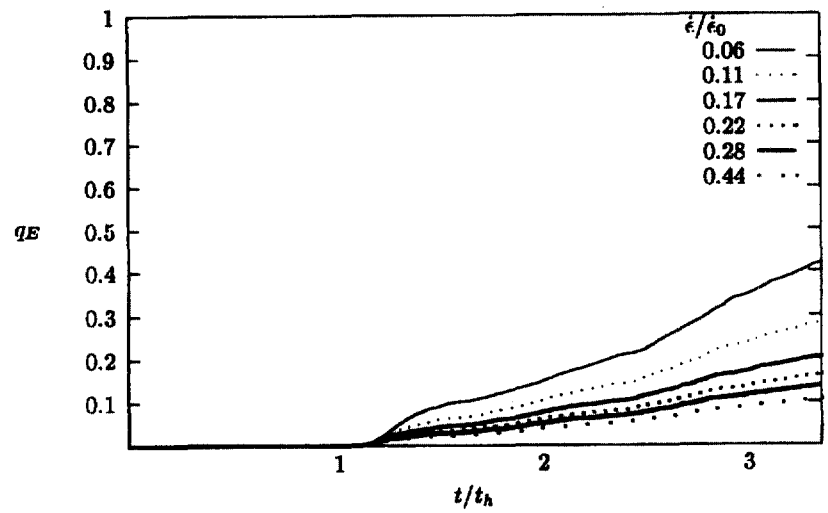

Fig. 11. Fraction of the externally imparted elastic strain energy that arrives to the bottom of the faulted specimen plotted vs. time for six strain rates.

In simulations the elastic energy E^{top} is imparted to the top of the specimen in the form of a strain pulse, defined as $\varepsilon(t) = a_0 \sin[\omega(t/t_h)]$, $0 \leqslant t/t_h \leqslant \pi(2\omega)$, where $t_h = c_0 L$ and c_0 are the time needed for an elastic wave to travel from the top to bottom of the pristine lattice and the speed of the elastic wave in the pristine lattice, respectively. The imparted strain rate is varied by changing the parameter ω within the range $(0.05\text{–}0.44)\omega_0$, where $\omega_0 = \pi c_0/2L$ is the lowest natural frequency of the pristine lattice. The specimen is extended at the bottom by a length L of a pristine lattice to avoid the influence of the reflected wave on the energy E^{bottom} recorded at the bottom of the actual lattice.

The fraction ($q_E = E^{\text{bottom}}/E^{\text{top}}$) of the imparted elastic strain energy that arrives to the bottom of the pristine lattice and the lattice containing the fault are plotted for six different strain rates vs time in Figs 10 and 11. The universality becomes obvious if the logarithm of the time (obtained combining data in Figs 10 and 11) needed for 10% of the imparted energy $q_E = 0.1$ to reach the bottom of the lattice is plotted (Fig. 12) vs the strain rate. With a very satisfactory accuracy the simulation data fall on a straight line in the $\log t_{0.1}$ vs $\log \dot{\varepsilon}$ space, indicating the "universality" of the proposed measure of the fault "width". The fault "width", which is proportional to the time lag, admits the simple scaling law

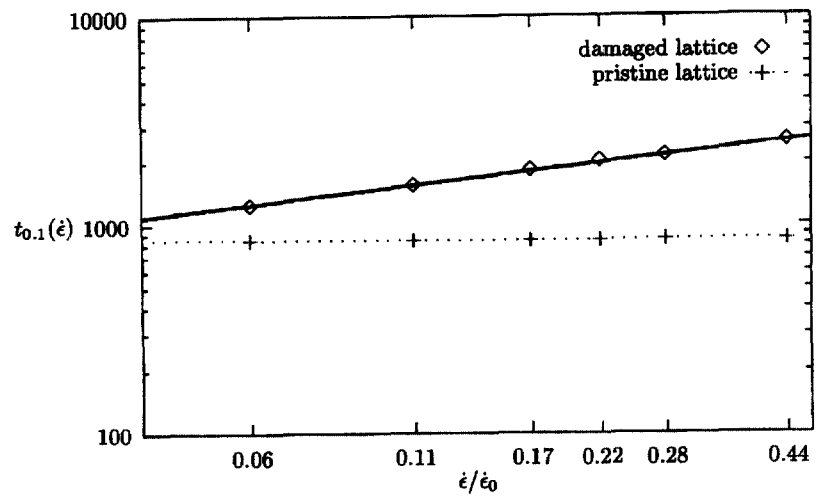

Fig. 12. The time needed for 0.1 of the imparted strain energy to arrive to the specimen bottom plotted (in logarithmic scale) vs. the rate at which the strain is applied. The slope fitted through the simulation data is 0.35. The dotted line corresponds to the pristine lattice.

$$w \propto (\dot{\epsilon})^{0.35} \tag{10}$$

demonstrating that some order can always be found lurking behind the apparent disorder.

The expression (10) implies that the band "width" vanishes in the static case. The reason why the "width" of the fault vanishes in a purely static approximation can be inferred from the "ant in the labyrinth" concept introduced by de Gennes (see Stauffer and Aharoni, 1992; Sahimi, 1994). Consider an ant (random walker) moving on a pristine lattice. Each step made by the ant is equivalent to a unit of time. The radial distance between the initial and current location of the ant is proportional to the square root of the time (number of steps) and the proportionality constant is the lattice diffusivity. If the ant walks on a disordered lattice which lacks a fraction of its bonds it must be assumed that the ant can move from the currently occupied node only to the nodes which are still connected to it by an extant link. The ant is "penalized" to remain stationary for a unit of time whenever it selects to relocate to a node which is not any more linked to its current location. In this case the distance between the initial and current positions traversed by the ant randomly walking within the damaged lattice is shorter than that traversed in a pristine lattice. However, in the limit of an infinitely long period the ant has an infinitely long time at its disposal and it will always be able to escape from a damaged region as long as it is connected by at least one link to the rest of the lattice. In other words, in a static approximation it is impossible to localize the strain energy as long as the fault is able to transmit stresses, i.e. as long as the specimen is connected and the floppy modes (during which the elastic energy of the system is constant) eliminated (Krajcinovic, 1996). It is, therefore, obvious that the zero "width" of the fault is the consequence of the static treatment of the dynamic phenomenon of the fault growth. Similar conclusions can be derived for the diffusion on and vibration of percolation lattices discussed at length in Stauffer and Aharoni (1992) and Sahimi (1994).

8. SUMMARY AND CONCLUSIONS

The proposed model emphasizes the qualitative (statistical) aspect of the faulting in particular and strain localization in general. It demonstrates the reasons why the traditional, continuum models provide a good estimate of the localization onset. Simultaneously, the simulation data clearly indicate that the application of deterministic models based on the mean field and continuum theories will often provide unreliable estimates of the deformation within the softening regime.

The discussion related to the band "width" shows that its vanishing value is not as pathological as originally thought. In fact, the "width" of the band will always be equal to zero in the limit of static behavior. Using the arguments of statistical physics the "effective width" of the fault is determined by the effect it has on the propagation of the elastic stresses through the specimen. The effect that the damage has on the rate of the stress propagation through a disordered lattice was defined by a simple scaling law (10). The measure of this "order" is reflected in the fit with which the simulation data follow the scaling law (10). Assuming that a more ambitious statical analysis will support the simulation data reported in this paper the proposed "measure" of the band "width" will provide a simple, accurate, robust and physically meaningful scaling law for a set of particular material defined by the equal distribution of link strengths.

Finally, it should be noted once more that the fit between the simulation data compiled in the course of this study and the test data is of qualitative nature. It would be conceptually simple to adjust the lattice parameters such as link stiffnesses and lengths to the material parameters and grain sizes of a particular rock, concrete, silicon or ceramics. However, the localization depends strongly on the dimensionality of the specimen. Unfortunately, particle dynamics simulations of three-dimensional lattices of a reasonably large size will take a better computational device than the one that was on the disposal of the authors of this study. There is little doubt that this hurdle will soon appear as being a vestige of a distant past.

Acknowledgements—The authors gratefully acknowledge the financial support of the Office of Basic Energy Sciences, U.S. Department of Energy and Engineering Science Division of the U.S. Army Research Office in the form of a research grant to the Arizona State University.

REFERENCES

Aifantis, E. C. (1984) On the microstructural origin of certain inelastic modes. *J. Engn. Mater. Technology* **106**, 326–334.

Allen, M. P. and Tildesley, D. J., *Computer Simulations of Liquids*. Clarendon Press, Oxford, U.K.

Anderson, P. W. (1958) Absence of diffusion in certain random lattices. *Phys. Rev.* **109**, 1492–1505.

Bazant, Z. P. and Cedolin, L. (1991) *Stability of Structures. Elastic, Inelastic Fracture and Damage Theories*. Oxford University Press, New York, NY.

Bazant, Z. P. and Pijaudier-Cabot, G. (1988) Nonlocal continuum damage, localization instability and convergence. *Journal of Applied Mechanics* **55**, 287–293.

Belytschko, T. and Lasry, D. (1989) Localization limiters and numerical strategies for strain-softening materials. In *Cracking and Damage, Strain Localization and Size Effect*, ed. J. Mazars and Z. P. Bazant, pp. 349–362. Elsevier Applied Science, London, U.K.

Belytschko, T., Moran, B. and Kulkarni, M. (1991) On the crucial role of imperfections in quasi-static viscoplastic solutions. *Journal of Applied Mechanics* **58**, 658–665.

Benallal, A., Billardon, R. and Geymonat, G. (1990) Phenomenes de localisation a la frontiere d'un solide. *C. R. Acad. Sci. Paris, Serie II.* **310**, 679–684.

Bigoni, D. and Hueckel, T. (1991) Uniqueness and localization—associative and non-associative elastoplasticity. *International Journal of Solids and Structures* **28**, 197–213.

Billardon, R. and Doghri, I. (1989) Localization bifurcation analysis for damage softening in elasto-plastic materials. In *Cracking and Damage, Strain Localization and Size Effect*, ed. J. Mazars and Z. P. Bazant, pp. 259–307. Elsevier Applied Science, London, U.K.

de Borst, R. (1991) Simulation of strain localization: a reappraisal of the Cosserat continuum. *Engng. Comput.* **8**, 317–332.

de Borst, R. and Muhlhaus, H. B. (1992) Gradient-dependent plasticity: formulation and algorithmic aspects. *International Journal of Numerical Methods in Engineering* **35**, 521–539.

Delaplace, A., Pijaudier-Cabot, G. and Roux, S. (1996) Progressive damage in discrete models and consequence on continuum Modeling. *Journal of the Mechanics and Physics of Solids* **44**, 99–136.

DiLellio, J. A. and Olmstead, W. E. (1997) Temporal evolution of shear band thickness. *Journal of the Mechanics and Physics of Solids* **45**, 345–359.

Finno, R. J., Harris, W. W., Mooney, M. A. and Viggiani, G. (1996) Strain localization and undrained steady state of sand. *J. Geotech. Engng.* **122**, 462–473.

Fleck, N. A. (1991) Brittle fracture due to an array of microcracks. *Proceedings of the Royal Society London A* **432**, 55–76.

Frantziskonis, G. and Loret, B. (1995) Scale dependent constitutive relations—information from wavelet analysis and application to localization problems. *Eur. J. Mech., A/Solid* **14**, 873–892.

Hallbauer, D. K., Wagner, H. and Cook, N. G. W. (1976) Some observations concerning the microscopic and mechanical behavior of quartzite specimens in stiff, triaxial compression tests. *Int. J. Rock Mech. Min. Sci. and Geomech. Abstracts* **10**, 713–726.

Hansen, A., Roux, S. and Herrmann, H. J. (1989) Rupture of central-force lattices. *J. Phys. France* **50**, 733–744.

Isichenko, M. B. (1992) Percolation, statistical topography and transport in random media. *Review of Modern Physics* **64**, 961–1043.

Isida, M. and Nemat-Nasser, S. (1987) On mechanics of crack growth and its effect on the overall response of brittle porous solids. *Acta metall.* **35,** 2887–2898.
Hill, R. (1963) Elastic properties of reinforced solids: some theoretical principles. *Journal of the Mechanics and Physics of Solids* **12,** 199–212.
Horii, H. and Nemat-Nasser, S. (1986) Brittle failure in compression: splitting, faulting and brittle–ductile transition. *Phil. Trans. Royal Soc. London* **319,** 337–374.
Jaeger, J. C. and Cook, N. G. W. (1979) *Fundamentals of Rock Mechanics*, 3rd edn. Chapman and Hall, London, U.K.
Jirasek, M. and Bazant, Z. P. (1995) Particle model for quasibrittle fracture and application to sea ice. *Journal of Engineering Mechanics, ASCE* **121,** 1016–1025.
Krajcinovic, D. (1996) *Damage Mechanics*. North-Holland, Amsterdam, The Netherlands.
Krajcinovic, D. (1997) Essential structure of damage mechanics theories. Theoretical and Applied Mechanics 1996. *Proceedings of the 19th International Congress of Theoretical and Applied Mechanics*. T. Tatsuni, E. Watanabe and T. Kambe, eds., pp. 411–426, North-Holland, Amsterdam.
Krajcinovic, D. and Basista, M. (1991) Rupture of central-force lattices revisited. *Journal of Physics I* **1,** 241–245.
Kreher, W. and Pompe, W. (1989) *Internal Stresses in Heterogeneous Solids*. Akademie-Verlag, Berlin, Germany.
Lockner, D. A. and Byerlee, J. D. (1992) Fault growth and acoustic emissions in confined granite. *Appl. Rev. Proc. 22nd Midwestern Mech. Conf.*, **45**(3), pp. S165–S173.
Lockner, D. A. and Madden, T. R. (1991) A multiple-crack model of brittle fracture. I. Non-time dependent *s* simulations. *J. Geophys. Res.* **96,** 19,623–19,642.
Lockner, D. A., Byerlee, J. D., Kuksenko, V., Ponomarev, A. and Sidorin, A. (1991) Quasi-static fault growth and shear fracture energy in granite. *Nature* **350**(6313), 39–42.
Loret, B. and Prevost, J. H. (1990) Dynamic strain localization in elasto-(visco)-plastic solids, Part 1. General formulation and one-dimensional examples. *Comp. Meth. Appl. Mech. and Engng.* **83,** 247–273.
Muhlhaus, H. B. and Aifantis, E. C. (1991) A variational principle for gradient plasticity. *International Journal of Solids and Structures* **28,** 845–858.
Muhlhaus, H. B. and Vardoulakis, I. (1987) The thickness of shear bands in granular materials. *Geotechnique* **37,** 271–283.
Needleman, A. (1988) Material rate dependence and mesh sensitivity in localization problems. *Comp. Methods in Appl. Mech. and Engng.* **67,** 69–85.
Needleman, A. (1989) Computational micromechanics. In *Theoretical and Applied Mechanics*, ed. P. Germain, M. Piau and D. Caillerie, pp. 217–240. Elsevier Science Publ., B.V. Amsterdam, The Netherlands.
Neilsen, M. K. and Schreyer, H. L. (1993) Bifurcation in elastic–plastic materials. *International Journal of Solids and Structures* **30,** 521–544.
Ortiz, M. (1989) Extraction of constitutive data from specimens undergoing strain localization. *Journal of Engineering Mechanics, ASCE* **115,** 1748–1760.
Ottosen, N. S. and Runesson, K. (1991) Properties of discontinuous bifurcation solutions in elasto-plasticity. *International Journal of Solids and Structures* **27,** 153–172.
Paterson, M. S. (1978) *Experimental Rock Deformation—the Brittle Field*. Springer-Verlag, Berlin, Germany.
Peric, D., Runesson, K. and Sture, S. (1993) Prediction of plastic localization using MRS-Lade model. *Journal of Geotechnical Engineering, ASCE* **119,** 639–661.
Reches, Z. and Lockner, D. A. (1994) Nucleation and growth of faults in brittle rock. *J. Geophys. Res.* **99**(B9), 18,159–18,173.
Rice, J. R. (1976) The localization of plastic deformation. In *Theoretical and Applied Mechanics*, ed. W. T. Koiter, pp. 207–220. North-Holland Publ. Co., Amsterdam, The Netherlands.
Rizzi, E. (1995) Sulla Localizzatione delle Deformazioni in Materiali e Strutture. Tesi di Doctorato di Ricerca. Dipartimento di Ingegneria Strutturale, Politecnico di Milano.
Roscoe, K. H. (1970) The influence of strain in soil mechanics, 10th Rankine Lecture. *Geotechnique* **20,** 129–170.
Rudnicki, J. W. and Rice, J. R. (1975) Conditions for the localization of deformation in pressure-sensitive materials. *Journal of the Mechanics and Physics of Solids* **23,** 371–394.
Sahimi, M. (1994) *Applications of Percolation Theory*. Taylor and Francis, Inc., Bristol, PA.
Sammis, G. C. and Ashby, M. F. (1986) The failure of brittle porous solids under compressive stress state. *Acta metall.* **34,** 511–526.
Schlangen, E. and van Mier, J. G. M. (1992) Micromechanical analysis of fracture of concrete. *International Journal of Damage Mechanics* **1,** 435–454.
Simo, J. C. (1989) Strain softening and dissipation: a unification of approaches. In *Cracking and Damage, Strain Localization and Size Effect*, ed. J. Mazars and Z. P. Bazant, pp. 440–461. Elsevier Applied Science, London, U.K.
Stauffer, D. and Aharony, A. (1992) *Introduction to Percolation Theory*. Taylor and Francis Inc., Bristol, PA.
Sulem, J. and Vardoulakis, I. (1990) Bifurcation analysis of the triaxial test on rock specimens. *Acta Mechanica* **83,** 195–212.
Torquato, S. (1991) Random Heterogeneous media: microstructure and improved bounds on effective properties. *Applied Mechanics Review* **44,** 37–76.
Triantafyllidis, N. and Aifantis, E. C. (1986) A gradient approach to localization of deformation. I. hyperelastic materials. *Journal of Elasticity* **16,** 215–237.
Tzschichholz, F., Herrmann, H. J., Roman, H. E. and Pfuff, M. (1994) Beam model for hydraulic fracturing. *Physics Review B* **49,** 7056–7059.
van Mier, J. G. M. (1984) Strain-softening under multiaxial loading conditions. Ph.D. thesis. Tech. Hogeschool Eindhoven, The Netherlands.
Vardoulakis, I. and Aifantis, E. C. (1994) On the role of microstructure in behavior of solids: effects of higher order gradients and internal intertia. *Mech. Mater.* **18,** 151–158.
Vardoulakis, I. and Graf, B. (1985) Calibration of constitutive models for granular materials using data from biaxial experiments. *Geotechnique* **35,** 299–317.
Vardoulakis, I., Graf, B. and Hettler, A. (1985) Shear band formation in a fine-grained sand. In *Proc. 5th Int. Conf. Numer. Meth. Geomech., Nagoya* 1, pp. 517–521. Balkema, Rotterdam, The Netherlands.
von Karman, T. (1911) Festigkeiteversuche unter allseitgem Druck. *Z. Ver. dt. Ing.*, **55,** 1749–1757.

Vujosevic, M. and Krajcinovic, D. (1997) Creep rupture of polymers: a statistical model. *International Journal of Solids and Structures* **34,** 1105–1122.

Wong, T.-F. (1990) Mechanical compaction and brittle–ductile transition in porous sandstones. In *Deformation Mechanisms, Rheology and Tectonics*, ed. R. J. Knipe and E. H. Rutter, pp. 111–122. Geological Soc. Spec. Publ. No. 54.

Wu, F. H. and Freund, L. B. (1984) Deformation trapping due to thermoplastic instability in one-dimensional wave propagation. *Journal of the Mechanics and Physics of Solids* **32,** 119–132.